ULTRA LOW COST ADAPTATIONS OF ELECTRO-MECHANICAL IMPEDANCE (EMI) TECHNIQUE FOR STRUCTURAL HEALTH MONITORING

Suresh Bhalla, Ashok Gupta, Sahil Bansal and Tarun Garg

Department of Civil Engineering, Indian Institute of Technology Delhi,

Hauz Khas, New Delhi 110 016 INDIA

ABSTRACT

This paper outlines new low-cost hardware set-ups as viable substitutes for conventionally employed cost-intensive impedance analyzers/ LCR meters for the implementation of electro-mechanical impedance (EMI) technique for SHM/ NDE. The proposed solutions warrant basic low-cost equipment, such as function generator and digital multimeter, which are commonly available. Unlike the conventional impedance analyzers/ LCR meters, only the absolute admittance (i.e. magnitude) is measured. A simple computational approach is outlined for effective utilization of the absolute admittance function for SHM after filtering the passive component. Comparison of results with LCR measurements shows that the measurement accuracy of the proposed set-up is fairly good, repeatability excellent, and the damage sensitivity comparable to that of the cost-intensive conventional hardware. The proposed adaptation is therefore a suitable candidate for the widespread industrial applications of the EMI technique.

KEYWORDS: Admittance, Electro-mechanical impedance (EMI) technique, low-cost, piezo-electric ceramic (PZT), multimeter, function generator.

INTRODUCTION

The EMI technique has made significant forays in the domains SHM and NDE during the last fifteen years. The technique began its journey in the early nineties emanating out the ground breaking work by Liang et al. (1994). Since then, extensive research efforts have been undertaken by several research groups worldwide on experimental as well as theoretical frontiers, aimed at widespread industrial dissemination of the technique. The technique is essentially based on monitoring the structural mechanical impedance via the electromechanical admittance signature of the surface bonded lead zirconate titanate piezoelectric-ceramic (PZT) patch, by utilizing its direct and converse piezoelectric properties simultaneously (Sun et al., 1995). The patch is subjected to an alternating voltage excitation through an impedance analyzer/ LCR meter, sweeping through a particular frequency range, generally 30 to 400 kHz. At a given frequency, the patch actuates the structure and the structural response is in-turn sensed and measured in terms of the electromechanical admittance of the patch, consisting of the real and the imaginary components, the conductance and the susceptance respectively. In this manner, frequency plots, termed conductance and susceptance signatures, are generated across the specified frequency range. Any change in the condition of the structure manifests itself as an alteration in these signatures, which is utilized for SHM and NDE, considering the signatures of the healthy state structure as the baseline.

During the initial years, the research efforts mainly focused on exploring the possible application of the EMI technique on various mechanical and structural systems, such as truss joints (Ayres et al., 1998), spot welded structural joints (Guirgiutiu et al., 1999),

composite masonry walls and pipe joints (Park et al., 2000), reinforced concrete prototype bridges (Soh et al., 2000), rehabilitated concrete members (Saffi and Sayyah, 2001), jet engine components (Winston et al., 2001) and aircraft body parts (Guirgiutiu et al., 2002). Thereafter, the focus shifted on modelling the structure-PZT interaction and damage quantification (Bhalla and Soh, 2003; 2004a; 2004b) and the effects of the adhesive bonding layer (Xu and Liu, 2002; Bhalla and Soh, 2004c). The hardware issues related to the EMI technique were first investigated by Peairs et al. (2004), who proposed a low-cost version of the EMI technique using a FFT analyzer. The work was further extended by Xu and Giurgiutiu (2005), Park et al. (2006) and Panigrahi et al. (2008).

This paper presents the results of recent efforts by the authors to reduce the hardware requirements for the real life implementation of the EMI technique to bare minimum while at the same time ensuring reasonable accuracy and damage sensitivity. The proposed approach, which warrants a simple function generator and a digital multimeter, is based on the measurement of absolute admittance function. The paper, therefore, first outlines a computational approach to extract the active part of the absolute admittance, followed by a description of the hardware set-up and its proof-of-concept implementation on a laboratory structure.

UTILIZATION OF ABSOLUTE ADMITTANCE FOR SHM

For a square PZT patch of length $2l$ and thickness h, surface-bonded on any structure, such as the one shown in Fig. 1, the complex electro-mechanical admittance can be expressed as (Bhalla and Soh, 2004a)

$$\overline{Y} = G + Bj = 4\omega\ j\frac{l^2}{h}\left[\overline{\varepsilon_{33}^{T}} - \frac{2d_{31}^2\overline{Y^E}}{(1-\nu)} + \frac{2d_{31}^2\overline{Y^E}}{(1-\nu)}\left(\frac{Z_{a,eff}}{Z_{s,eff}+Z_{a,eff}}\right)\overline{T}\right] \quad (1)$$

where d_{31} is the piezoelectric strain coefficient, $\overline{Y^E} = Y^E(1+\eta j)$ the complex Young's modulus of the PZT patch at constant electric field and $\overline{\varepsilon_{33}^T} = \varepsilon_{33}^T(1-\delta j)$ the complex electric permittivity of the PZT material at constant stress (with η and δ denoting the mechanical and the dielectric loss factors respectively), ω the angular frequency, υ the Poisson's ratio, $j = \sqrt{-1}$ and $Z_{s,eff}$ and $Z_{a,eff}$ respectively the effective drive point mechanical impedance of the host structure and the PZT patch. The term $\overline{T}$ is the complex tangent ratio, given by

$$\overline{T} = \frac{1}{2}\left(\frac{\tan C_1\kappa l}{C_1\kappa l} + \frac{\tan C_2\kappa l}{C_2\kappa l}\right) \quad (2)$$

where κ represents the complex wave number. The coefficients C_1 and C_2, which are determined from the free PZT patch's signatures (before bonding it to the host structure), are supposed to empirically model the deviation of the PZT patch from the ideal behaviour. It is clear from Eq. (1) that any change in $Z_{s,eff}$ resulting from damage will alter the resulting admittance signature, which is utilized as the main damage indicator in the EMI technique.

During the early years, only the real component (G) was considered for SHM/ NDE (Sun et al., 1995; Park et al., 2003). The imaginary component, drowned by the capacitive contribution of the PZT patch, was considered redundant. Bhalla and Soh (2003)

demonstrated that the imaginary component can also be rendered equally sensitive by decomposing the admittance function as

$$\overline{Y} = \overline{Y}_P + \overline{Y}_A \tag{3}$$

with $\overline{Y_P} = 4\omega j \frac{l^2}{h}\left[\overline{\varepsilon_{33}^T} - \frac{2d_{31}^2 \overline{Y^E}}{(1-\nu)}\right]$ and $\overline{Y_A} = \frac{8\omega d_{31}^2 \overline{Y^E} l^2}{h(1-\nu)}\left(\frac{Z_{a,eff}}{Z_{s,eff} + Z_{a,eff}}\right)\overline{T}\, j$ (4)

The component $\overline{Y_P}$, which solely depends on the parameters of the PZT patch (and therefore unaffected by damage to the structure) was termed the 'passive' component by Bhalla and Soh (2003). $\overline{Y_A}$, which on the other hand, represents the contribution arising from structure-PZT interaction, was termed the 'active' component. $\overline{Y_P}$ can be broken down into real and imaginary parts as

$$\overline{Y_P} = G_P + B_P j \tag{5}$$

where $G_P = \frac{4\omega l^2}{h}\left\{\delta\varepsilon_{33}^T + K\eta\right\}$ and $B_P = \frac{4\omega l^2}{h}\left\{\varepsilon_{33}^T - K\right\}$ (6)

and $$K = \frac{2d_{31}^2 Y^E}{(1-\nu)} \tag{7}$$

The passive component can be filtered off from the raw signatures and the active components, G_A and B_A deduced as

$$G_A = G - G_P \tag{8}$$

and $$B_A = B - B_P \tag{9}$$

In this manner, by separating out the passive component, the damage detection sensitivity of the susceptance signature was shown to be elevated to a level comparable to that of the conductance signature (Bhalla et al., 2002; Bhalla and Soh, 2003). Recently, Kim et al. (2007) employed susceptance in addition to conductance for damage identification.

From the active conductance and susceptance, the absolute active admittance can be computed as

$$|Y_A| = \sqrt{G_A^2 + B_A^2} \tag{10}$$

In this paper, the possibility of utilizing $|Y_A|$ (which is obtainable from the proposed low-cost hardware set-up) is investigated for SHM. Fig. 1 shows the test specimen, an aluminium block of dimensions 50x48x10mm, instrumented with a PZT patch, 10x10x0.3mm in size, conforming to grade PIC 151 (PI Ceramic, 2008). The conductance (G) and susceptance (B) signatures of the patch were measured in the frequency range 40-90 kHz using HP 4192A impedance analyzer (Agilent Technologies, 2008). Thereafter, damage was induced in the specimen by drilling two holes of 5mm diameter, as shown in the figure. Fig. 2 shows the effect of the damage on G, B and the $|Y|$ ($= \sqrt{G^2 + B^2}$). It can be appreciated from the figure that whereas observable changes can be noticed in the plot of G, only negligible alterations appear in the plots of B and $|Y|$. Active components were then determined using Eqs. (8), (9) and (10). Fig. 3 shows the influence of the damage on the active components of susceptance and absolute admittance, i.e. B_A and Y_A respectively. Contrary to the previous observations, the damage is very clearly identifiable from the two plots. It may also be noted that for all practical purposes, the magnitudes of B_A and Y_A are more or less identical, due to the fact that $G_A << B_A$ (see Eq. 10). The significant improvement in damage sensitivity by using the active components is further highlighted by Fig. 4, which shows the root mean square deviation (RMSD) for six candidate parameters, namely G, B, $|Y|$, $|Z| = |Y|^{-1}$, B_A and $|Y_A|$, computed using

$$RMSD = \sqrt{\frac{\sum_{j=1}^{N}\left(G_j^1 - G_j^0\right)^2}{\sum_{j=1}^{N}\left(G_j^0\right)^2}} \tag{11}$$

where G_j^1 is the post-damage conductance/ or susceptance/ admittance/ impedance at the j^{th} frequency and G_j^0 the corresponding pre-damage severity value. It is observed from the figure that considering the active component substantially improves the damage sensitivity of B and $|Y|$. In the technique presented in this paper, only the absolute admittance $|Y|$ $(=\sqrt{G^2+B^2})$ is measured, without any information of the phase (and hence the components G and B). Therefore, as a simplification, taking into consideration the fact that $G_A << B_A$, the active component is computed as

$$\left|Y_A\right| \approx Y - Y_P \tag{12}$$

The next section outlines new low-cost hardware adaptations of the EMI technique with access to the measurement of the absolute admittance $|Y|$ only. From the knowledge of the PZT parameters, $|Y_A|$ can be determined using Eq. (12) and suitably employed for SHM.

NEW HARDWARE ADAPTATIONS OF EMI TECHNIQUE

Conventionally, the EMI technique employs impedance analyzer (or the LCR meter), which typically costs in the range of $20, 000 to $41, 000. Peairs et al. (2004) proposed a low cost electrical admittance measurement technique based on FFT analyzer (which typically costs $10, 000) in place of the impedance analyzer. Fig. 5 shows the electrical circuit employed by Peairs and co-workers. It essentially consisted of a small resistance

(<200Ω), connected in series with the PZT patch bonded to the structure (to be monitored). Upon applying an input voltage $\overline{V_i}$ across the combination through the FFT analyzer, the electric current $\bar{I}$ flows through the circuit, as given by

$$\bar{I} = \frac{\overline{V_o}}{R} \tag{13}$$

where $\overline{V_o}$ is the output voltage across the sensing resistor *R*, fed into the measurement channel of the FFT analyzer. Taking into consideration the fact that the electrical impedance of the PZT patch is very large as compared to that of the resistor *R*, the coupled electro-mechanical admittance $\bar{Y}$ of the bonded patch can be approximated as

$$\bar{Y} \approx \frac{\bar{I}}{\overline{V_i}} = \frac{\overline{V_o}}{R\overline{V_i}} \tag{14}$$

The measurement of the phase difference between $\overline{V_o}$ and $\overline{V_i}$ enabled the determination of the real and the imaginary components, *G* and *B* of $\bar{Y}$. This measurement approach was definitely cost-effective than the conventional impedance analyzer based approach. However, it involved the fast Fourier transform (FFT) of the time domain data, unlike the steady state measurements of impedance analyzer or LCR meter. Therefore, it faced bandwidth restrictions and could not be relied upon for frequencies greater than 100 kHz. Xu and Giurgiutiu (2005) made further improvement by utilizing a pair of function generator and a data acquisition (DAQ) card in place of the FFT analyzer and employing a sweep signal in place of chirp. However, their technique still necessitated FFT of the response spectrum. Park et al. (2006) made further breakthrough with the development of a miniaturized wireless sensor node using a low-cost integrated circuit chip that could measure and record the electrical impedance of the PZT patch, a microcontroller which

performed local computing, and a wireless telemetry which transmitted the signal wirelessly. However, the measurement from the sensor node differed several times in magnitude from the impedance analyzer.

Panigrahi et al. (2008) proposed an alternative measurement approach in the basic framework of Peair's circuit, using a pair of function generator (to produce $\overline{V_i}$) and a mixed signal oscilloscope (to measure $\overline{V_o}$, together costing about $5000. The main salient feature of the approach was the execution of steady state quasi sweep measurement (step-by-step excitation) emulating the high fidelity impedance analyzer/ LCR meter. This alleviated the requirement of FFT, enhanced the bandwidth and improved the measurement accuracy. The present paper extends the work of Panigrahi et al. (2008) aiming at further cost cuts while ensuring steady state quasi sweep measurements similar to an impedance analyzer. Two low-cost adaptations are demonstrated (a) transfer impedance approach, using an actuator-sensor pair; and (b) self impedance approach, using a single PZT patch. Both adaptations use the same basic equipment. The hardware solutions proposed in this paper warrants bare minimum equipment costing less than $2500 only.

Transfer Impedance Approach

Fig. 6 shows the circuit employed and Fig. 7 the hardware arrangement for the transfer impedance approach. Two PZT patches, one acting as a sensor and the other as an actuator, are bonded on the test specimen, an aluminium beam of dimensions 235x23x3mm, near the two ends. A sinusoidal voltage signal of 5 volts rms was applied at a frequency of 150 kHz across the actuator patch using the function generator (FG) model 702C (μ-TEC Electronic Measuring Instruments). The resulting voltage generated across the sensor patch was directly measured using digital multimeter (DMM) model Agilent 34411A (Agilent Technologies, 2008) without any conditioning circuit. The frequency was varied from 150 kHz to 160 kHz at an interval of 0.25 kHz to obtain a plot of gain (ratio of the magnitudes of the output and the input voltages) vs frequency, similar to conductance signature. This process of quasi-sweep measurements was implemented in GUI based VEE- PRO (Agilent Technologies, 2008) environment, as illustrated in Fig. 8. However, the use of the software is optional and alternatively the measurements can be stored in the memory of the DMM and retrieved later in a computer. The measurement was repeated three times with the three plots shown in Fig. 9(a), which demonstrate good repeatability. Damage was then induced in the beam by drilling a 5mm diameter hole in the middle (see Fig. 7b) and the gain measurement plot was again recorded three times, as shown in Fig. 9(b). Fig. 10 compares the average gain plots for the pristine and the damaged structures. Damage can be easily identified from the significant deviation observed in the plot of gain. The RMSD between the averaged plots was worked out as 65.34%. This is significantly higher than an averaged RMSD of 4.6% between the multiple measurement sets shown in Fig. 9.

Self Impedance Approach

The self-impedance approach employs the circuit of shown in Fig. 11 with Fig. 12 showing the actual experimental set-up. It is essentially Peair's approach with the difference that in place of the FFT analyzer, FG 702C is used to generate sinusoidal signals (5 volts rms). On the measurement front, DMM 34411A is used to measure the output voltage. The measurements were conducted on the same specimen which was used for the transfer impedance approach and against the same damage. The operations were controlled automatically in the VEE PRO 8.0 environment. However, unlike the technique of Peairs et al. (2004), the DMM only measured the absolute value of the output voltage, thereby only facilitating the determination of $|Y|$ (against G and B separately). Fig. 13 (a) shows the baseline measurements across a frequency range of 150-160 kHz, obtained by the proposed set-up, for three measurement sets, and Fig. 13 (b) similarly those for the post damage scenario. Excellent repeatability is very clearly apparent from Figs. 13(a) and (b), again substantiated by the fact that average RMSD was worked out to be 0.086% only. Figs. 14 (a) and (b) compare the averaged signatures with those acquired by means of LCR meter (model E4980, Agilent Technologies, 2008). It is observed that the measurements of the proposed set-up match those of the LCR meter. Average error was found to be within 7%. The only difference that exists between the two measurements is a vertical shift, which is most likely introduced by the cables. This error is not very significant in view of the fact that the EMI technique essentially focuses on "deviation" in the signatures rather than the absolute values.

Active admittance signatures were worked out using Eq. (12) for the LCR meter and the FG-DMM combination. Fig. 15(a) compares the active admittance signatures before and after damage obtained using LCR meter. Fig. 15(b) similarly provides the corresponding comparison for the measurements from the proposed hardware solution. It is observed that the proposed system can capture the damage quite reasonably well. Fig. 16 shows the computation of the RMSD for the LCR meter and the proposed low-cost hardware solution between the pre-damage and the post-damage scenarios, computed using Eq. (11). It is evident the proposed low-cost self-impedance hardware can detect damage reasonably well as compared to the measurements based on the conventional cost-intensive LCR meter. Similarly, the RMSD for the transfer impedance approach, computed as 65%, is significant enough as compared to noise related fluctuations (4.6%) From Figs. 15 and 16, a greater deviation may be noticed in the case of the measurements from the proposed set-up, though this fact cannot be generalized. Thus, the proposed hardware solutions are equally capable of damage detection, though they cost nearly one-eighth of an LCR meter and about one-sixteenth of an impedance analyzer.

CONCLUSIONS

This paper has proposed and experimentally demonstrated two low-cost hardware adaptations of the EMI technique. The proposed hardware solution warrants an investment less than $2500 only. The admittance measurements are conducted in quasi-sweep manner similar to the high fidelity impedance analyzer/ LCR meter. Although the approach only measures the absolute admittance, the active component extracted via the elimination of the passive component captures the essential damage sensitive features.

Comparison with the conductance measurements using the LCR meter demonstrates that the technique has fairly good measurement accuracy, excellent repeatability and competitive damage sensitivity. In addition, step-by-step steady state measurements ensure enhanced bandwidth and greater accuracy. The same set of hardware can be used in transfer impedance fashion based on the measurement of gain across an actuator-sensor pair. The transfer impedance approach provides greater sensing range and hence can supplement the self-impedance approach. The proposed solution is a low-cost alternative with potential for widespread industrial applications of the EMI technique ensuring competitive performance.

REFERENCES

Agilent Technologies. 2008. Test and Measurement Catalogue, USA.

Ayres, J. W., Lalande, F., Chaudhry, Z. and Rogers, C. A. 1998. "Qualitative Impedance-Based Health Monitoring of Civil Infrastructures", *Smart Materials and Structures*, 7(5): 599-605.

Bhalla, S., Naidu, A. S. K. and Soh C. K. 2002. "Influence of Structure-Actuator Interactions and Temperature on Piezoelectric Mechatronic Signatures for NDE", *Proc. of ISSS-SPIE International Conference on Smart Materials, Structures and Systems*, 12-14 December, Bangalore, 213-219.

Bhalla, S. and Soh, C. K. 2003. "Structural Impedance Based Damage Diagnosis by Piezo-Transducers", *Earthquake Engineering and Structural Dynamics*, 32(12):1897-1916.

Bhalla, S. and Soh, C.K. 2004a. "Structural Health Monitoring by Piezo-Impedance Transducers: Modeling", *Journal of Aerospace Engineering*, ASCE, 17(4):154-165.

Bhalla, S. and Soh, C.K. 2004b. "Structural Health Monitoring by Piezo-Impedance Transducers: Applications", *Journal of Aerospace Engineering*, ASCE, 17(4):166-175.

Bhalla, S. and Soh, C. K. 2004c. "Impedance Based Modeling for Adhesively Bonded Piezo-Transducers", *Journal of Intelligent Material Systems and Structures*, 15(12):955-972.

Giurgiutiu, V., Reynolds, A. and Rogers, C. A. 1999. "Experimental Investigation of E/M Impedance Health Monitoring for Spot-Welded Structural Joints", *Journal of Intelligent Material Systems and Structures*, 10(10):802-812.

Giurgiutiu, V. and Zagrai, A. N. 2002. "Embedded Self-Sensing Piezoelectric Active Sensors for On-Line Structural Identification", *Journal of Vibration and Acoustics*, ASME, 124:116-125.

Kim, J., Grisso, B. L., Ha, D. S. and Inman, D. J. 2007. "An All-Digital Low-Power Structural Health Monitoring System", *Proc. IEEE Conference on Technologies for Homeland Security*, Woburn, MA, 123-128.

Liang, C., Sun, F. P. and Rogers, C. A. 1994. "Coupled Electro-Mechanical Analysis of Adaptive Material Systems- Determination of the Actuator Power Consumption and System Energy Transfer", *Journal of Intelligent Material Systems and Structures*, 5(1):12-20.

Panigrahi, R., Bhalla, **S.** and Gupta, A. 2008. "A Cost-Effective Variant of Electromechanical Impedance Technique for Structural Health Monitoring", *Experimental Techniques*, in press.

Park, G., Cudney, H. H. and Inman, D. J. 2000. "Impedance-Based Health Monitoring of Civil Structural Components", *Journal of Infrastructure Systems*, ASCE, 6(4):153-160.

Park, G., Sohn, H., Farrar, C. R. and Inman, D. J. 2003. "Overview of Piezoelectric Impedance-Based Health Monitoring and Path Forward", *The Shock and Vibration Digest*, 35(5):451-463.

Park, G., Overly, T.G., Nothnagel, M. J., Farrar, C. R., Mascarenas, D. M., Todd, M. D. 2006. "A Wireless Active-Sensor Node for Impedance-based Structural Health Monitoring", *Los Alamos National Laboratory*, LA-UR-06-5735, Los Alamos, NM,

Peairs, D. M., Park, G. and Inman, D. J. (2004), "Improving Accessibility of the Impedance-Based Structural Health Monitoring Method", *Journal of Intelligent Material Systems and Structures*, 15(2):129-139.

PI Ceramic .2008. *Product Information Catalogue*, Lindenstrabe, Germany, http://www.piceramic.de.

Saffi, M. and Sayyah, T. 2001, "Health Monitoring of Concrete Structures Strengthened with Advanced Composite Materials Using Piezoelectric Transducers", *Composites Part B: Engineering*, 32(4):333-342.

Soh, C. K., Tseng, K. K. H., Bhalla, S. and Gupta, A. 2000, "Performance of Smart Piezoceramic Patches in Health Monitoring of a RC Bridge", *Smart Materials and Structures*, 9(4):533-542.

Sun, F. P., Chaudhry, Z., Rogers, C. A., Majmundar, M. and Liang, C. 1995. "Automated Real-Time Structure Health Monitoring via Signature Pattern Recognition", *Proc. SPIE Conference on Smart Structures and Materials,* San Diego, California, Feb.27-Mar1, 2443:236-247.

Winston, H. A., Sun, F. and Annigeri, B. S. 2001. "Structural Health Monitoring with Piezoelectric Active Sensors", *Journal of Engineering for Gas Turbines and Power*, ASME, 123(2):353-358.

Xu, B. and Giurgiutiu, V. 2005. "A Low-Cost and Field Portable Electromechanical (E/M) Impedance Analyzer for Active Structural Health Monitoring" *Proc. 5th International Workshop on Structural Health Monitoring,* Stanford University, September 15-17.

Xu, Y. G. and Liu, G. R. 2002. "A Modified Electro-Mechanical Impedance Model of Piezoelectric Actuator-Sensors for Debonding Detection of Composite Patches", *J. Intelligent Material Systems and Structures*, 13(6), 389-396.

LIST OF FIGURES

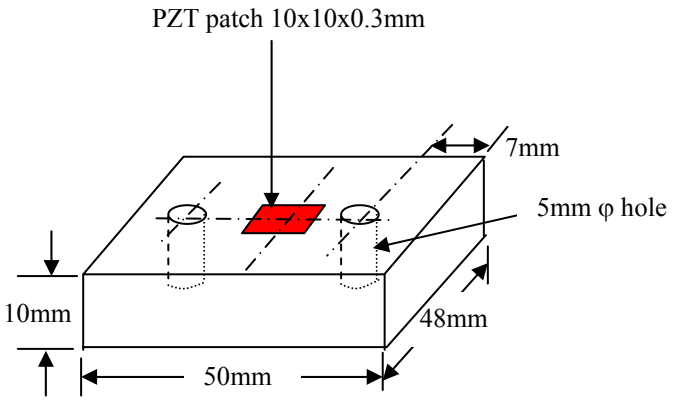

Fig. 1 A test specimen.

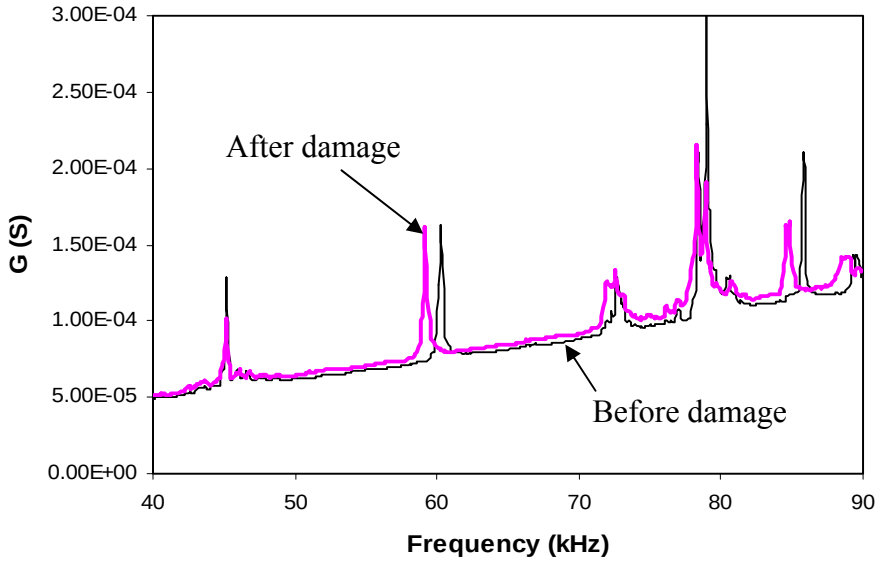

(a)

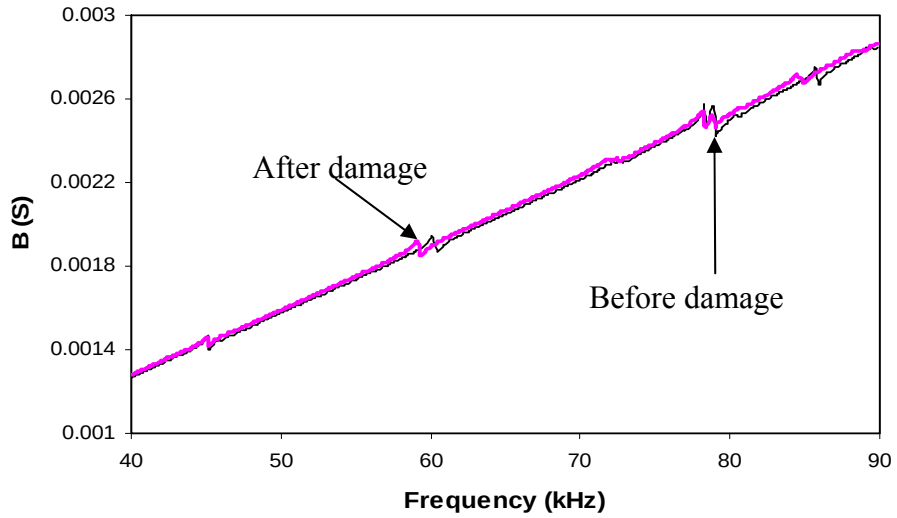

(b)

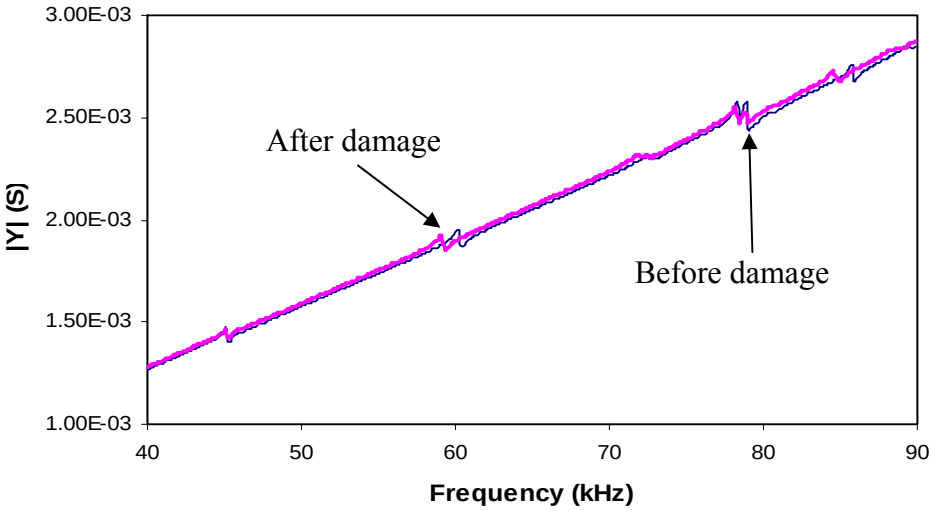

(c)

Fig. 2 Effect of damage on
(a) Conductance (b) Susceptance (c) Absolute admittance

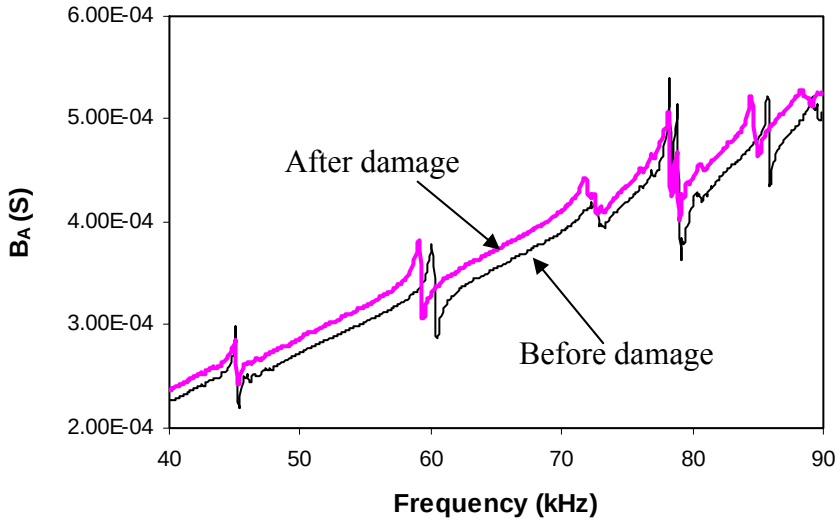

(a)

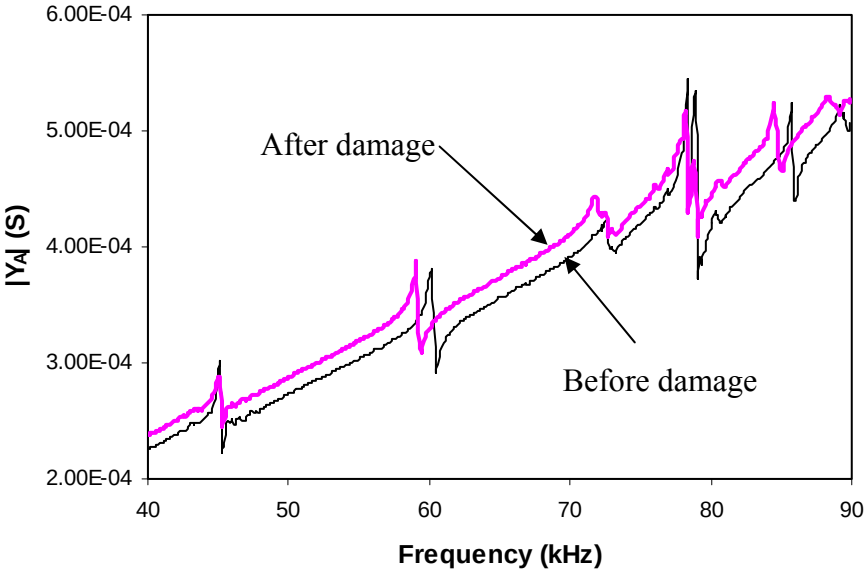

(b)

Fig. 3 Effect of damage on
(a) Active susceptance (b) Active absolute admittance

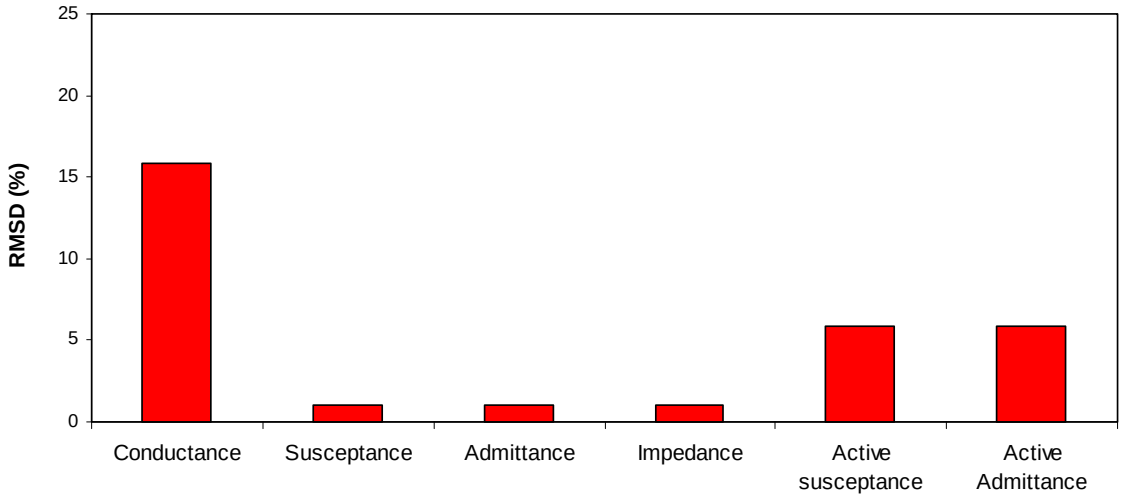

Fig. 4 Comparison of damage sensitivity of various parameters.

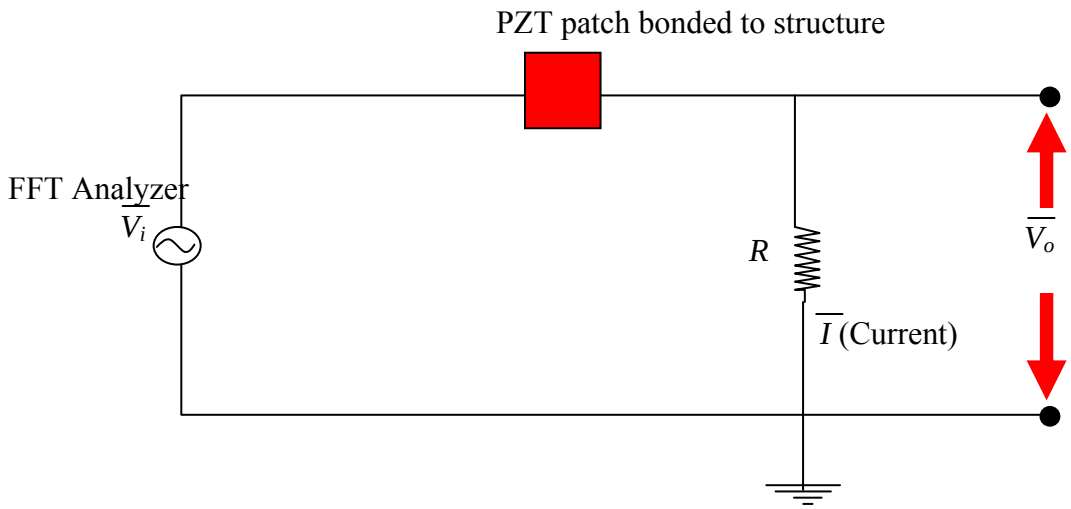

Fig. 5 Circuit employed by Peairs et al. (2004).

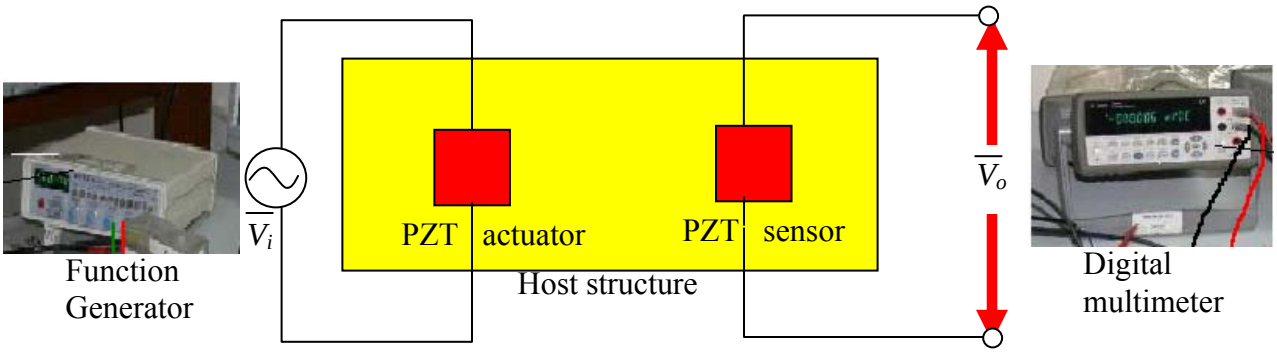

Fig. 6 Proposed circuit for transfer impedance approach.

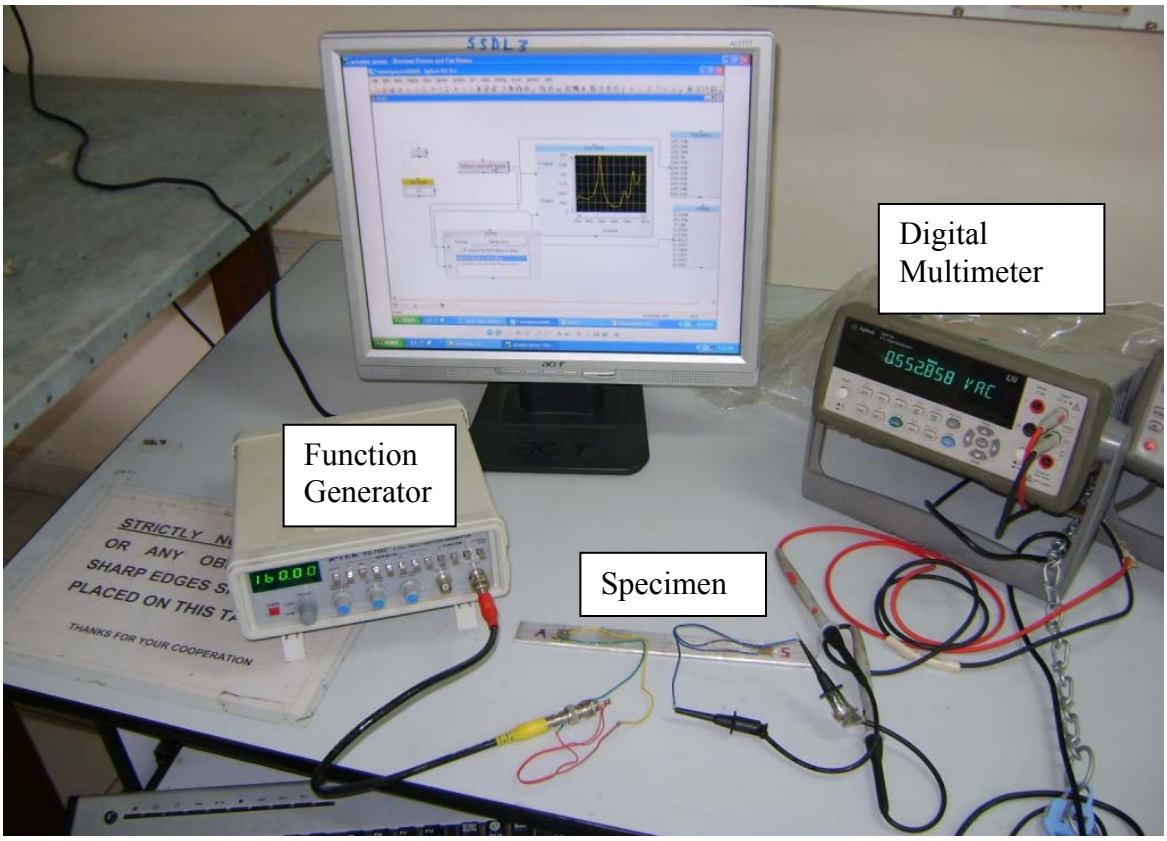

(a)

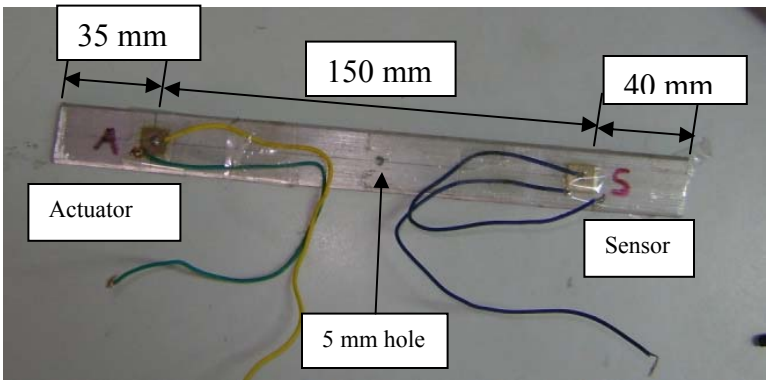

(b)

Fig. 7 Transfer impedance approach using FG and DMM.
(a) Experimental set-up (b) Specimen details

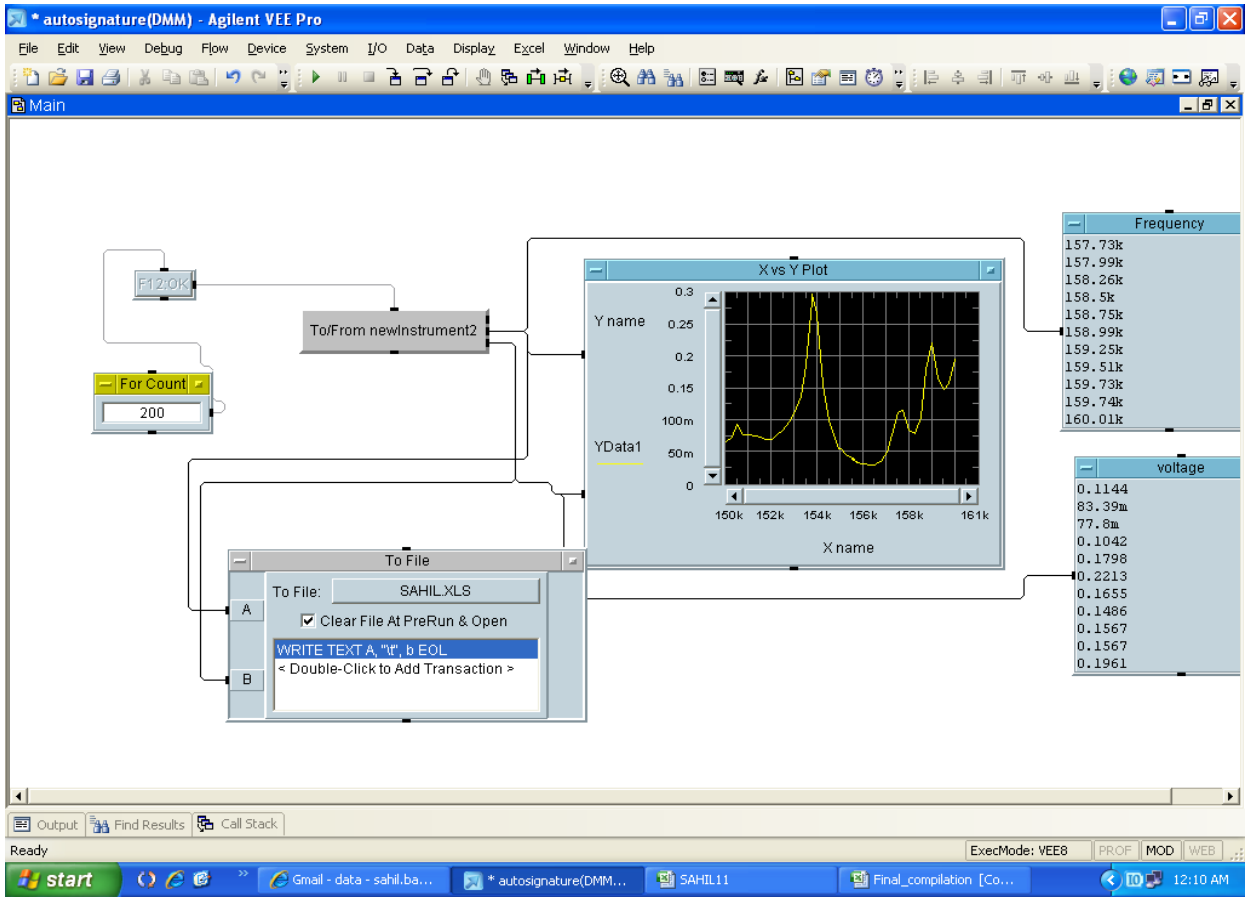

Fig. 8 Software interface in the proposed approach.

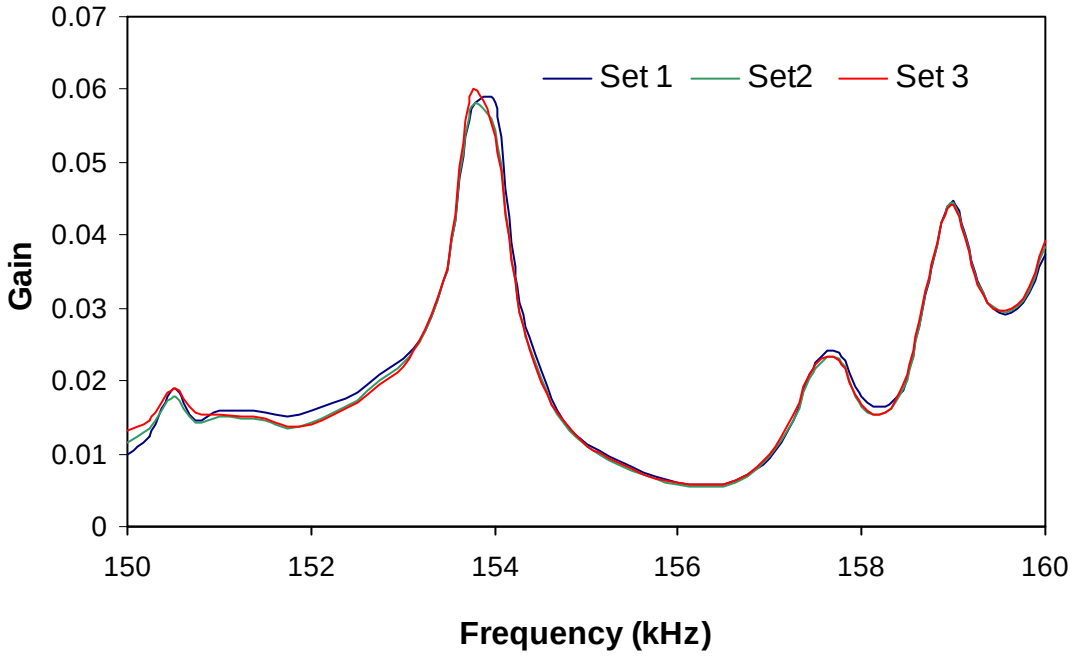

(a)

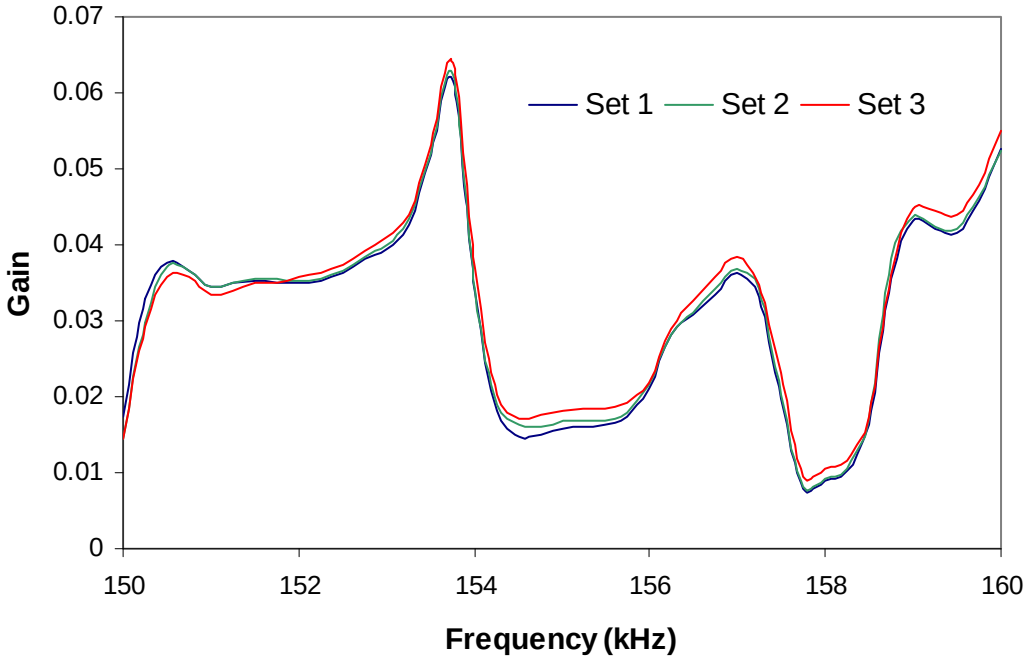

(b)

Fig. 9 Measurement using transfer impedance approach.
(a) Before damage (b) After damage

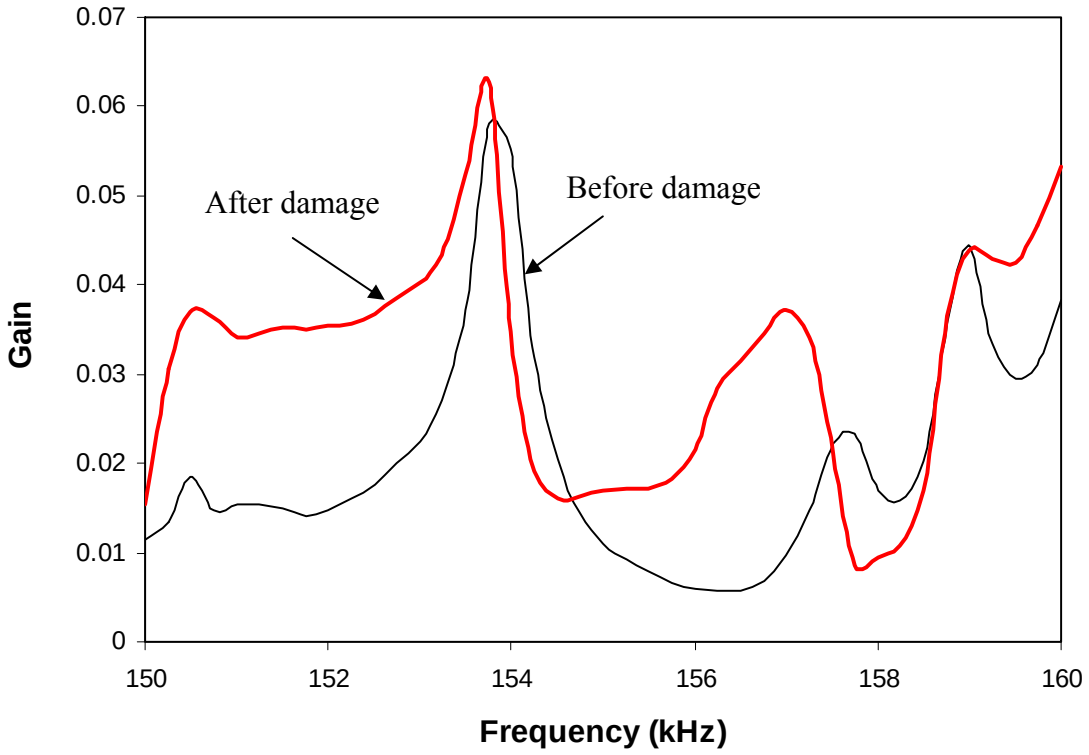

Fig. 10 Signatures before and after damage using the transfer impedance approach.

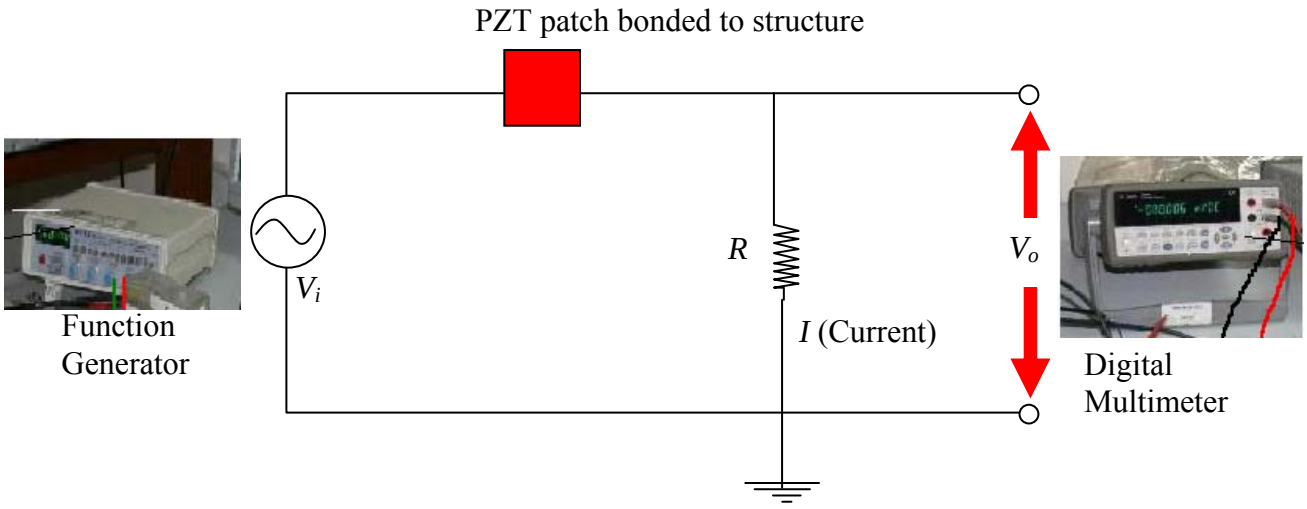

Fig. 11 Proposed circuit for self impedance approach.

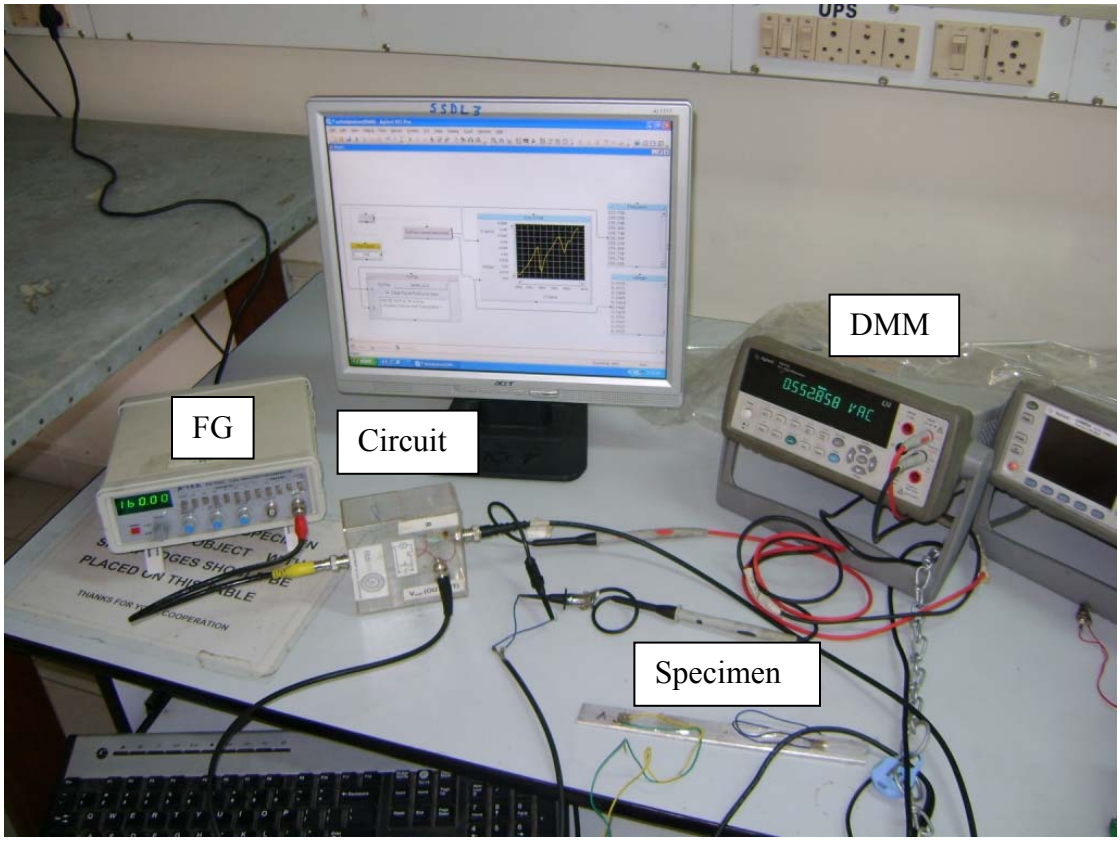

Fig. 12 Experimental set up for self impedance approach.

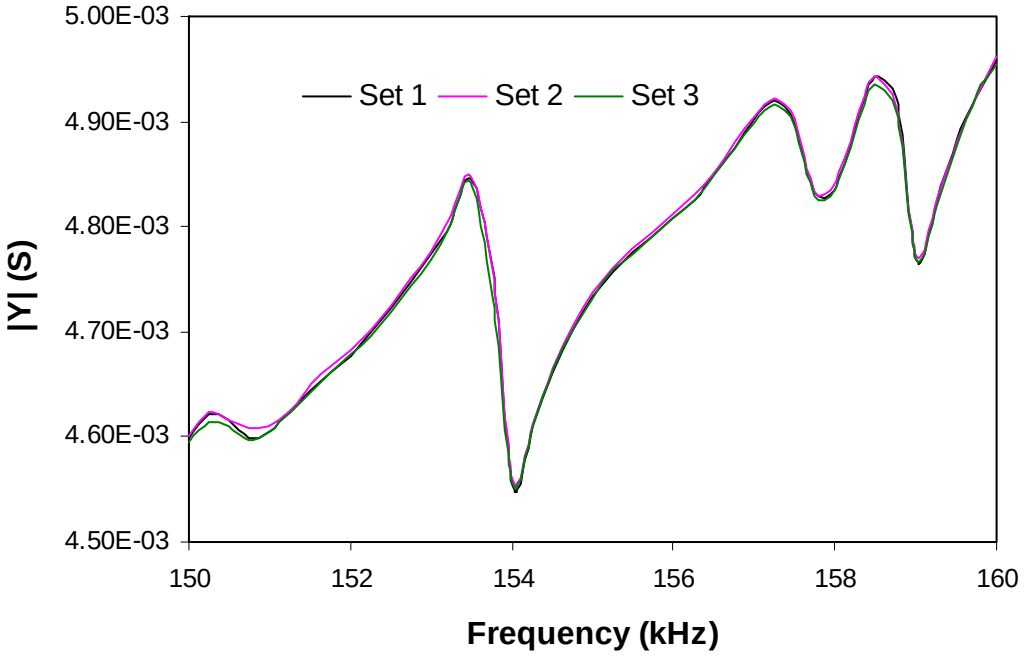

(a)

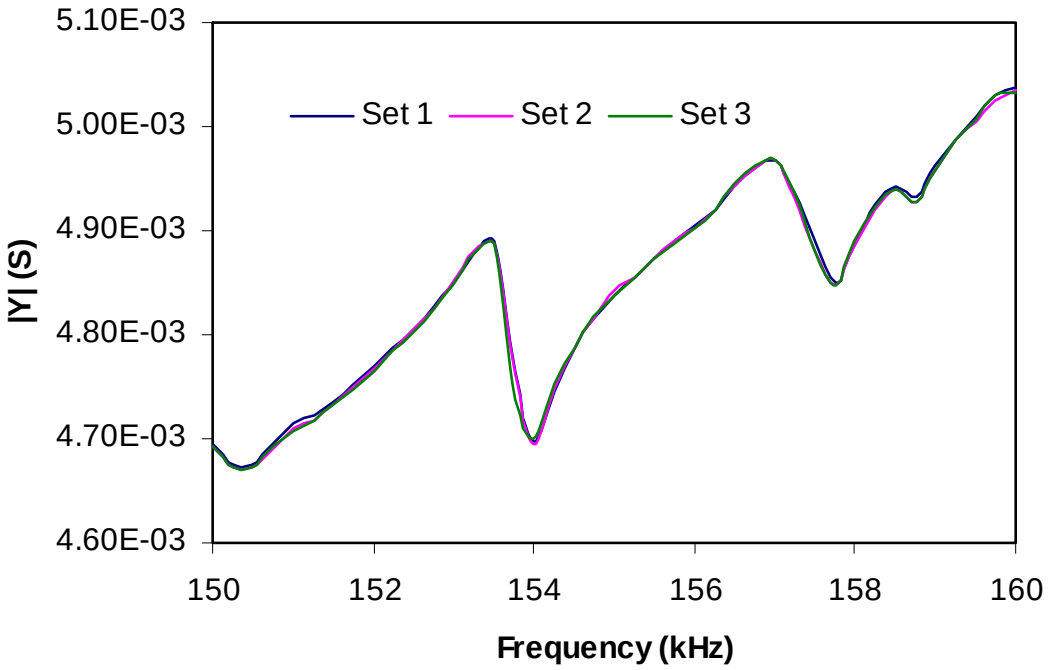

(b)

Fig. 13 Measurement using self impedance approach.

(a) Before damage (b) After damage

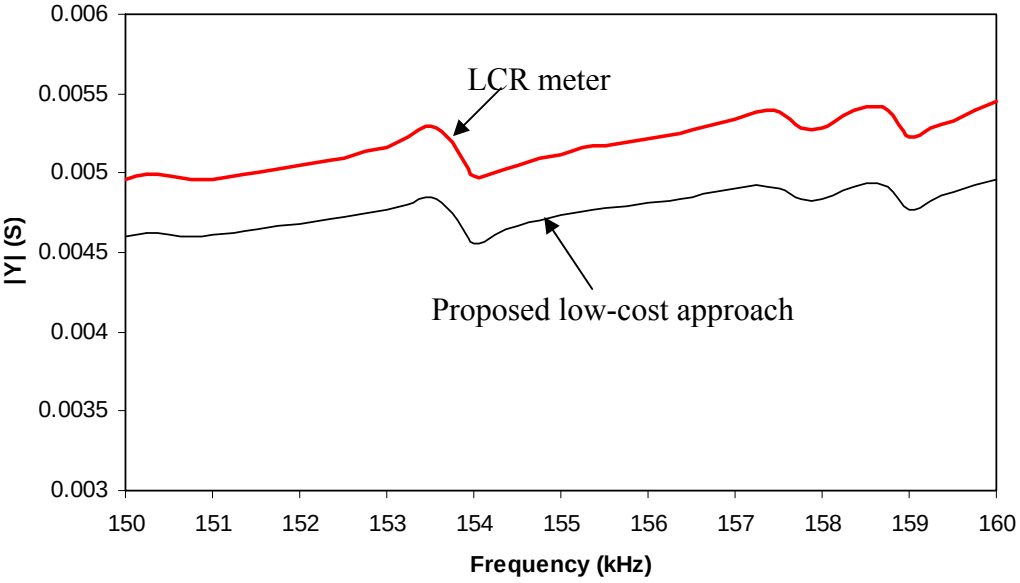

(a)

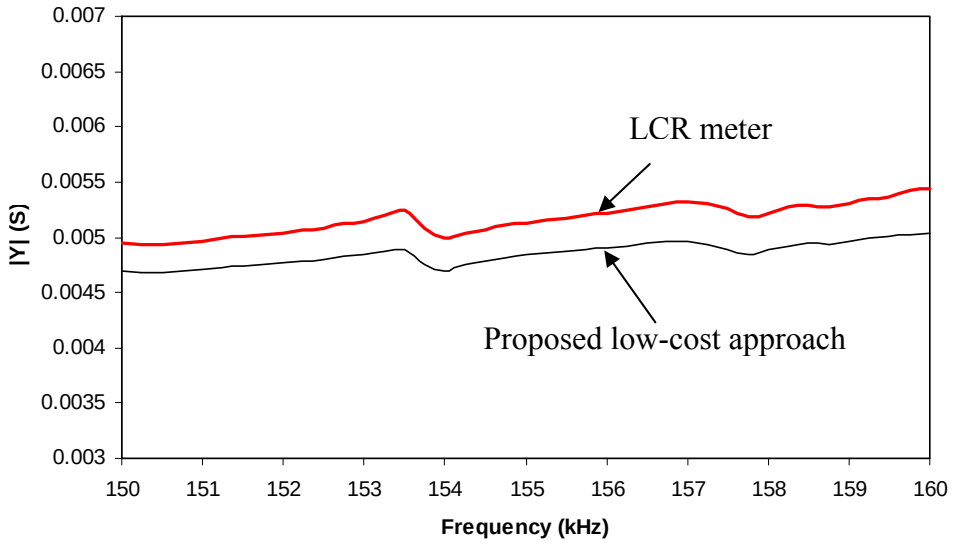

(b)

Fig. 14 Comparison of active admittance signatures obtained using LCR meter and proposed low-cost set-up. (a) Before damage (b) After damage

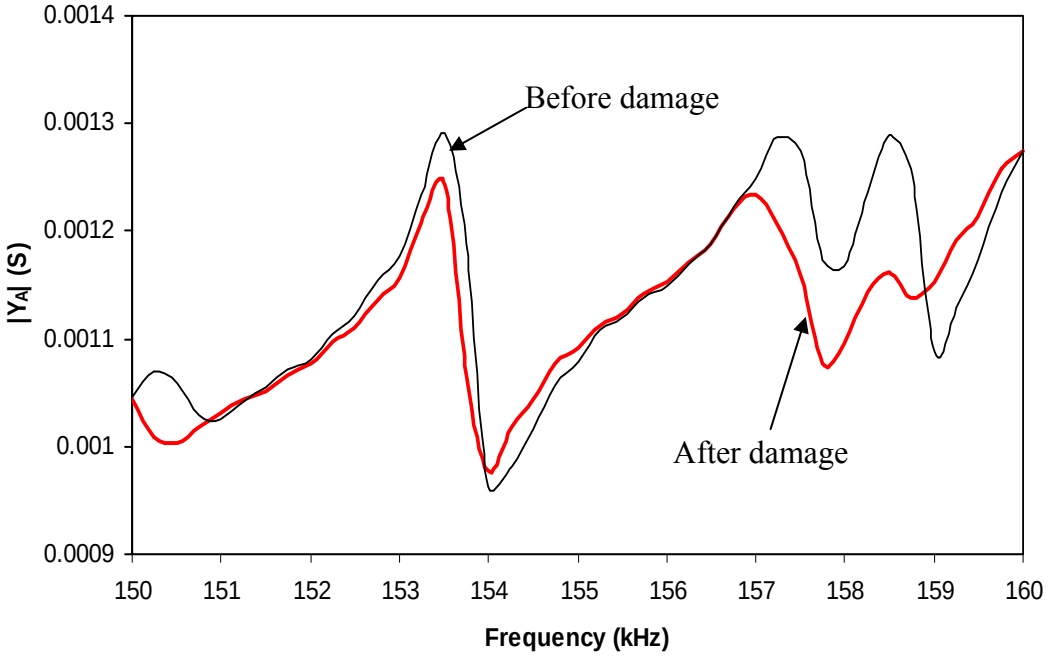

(a)

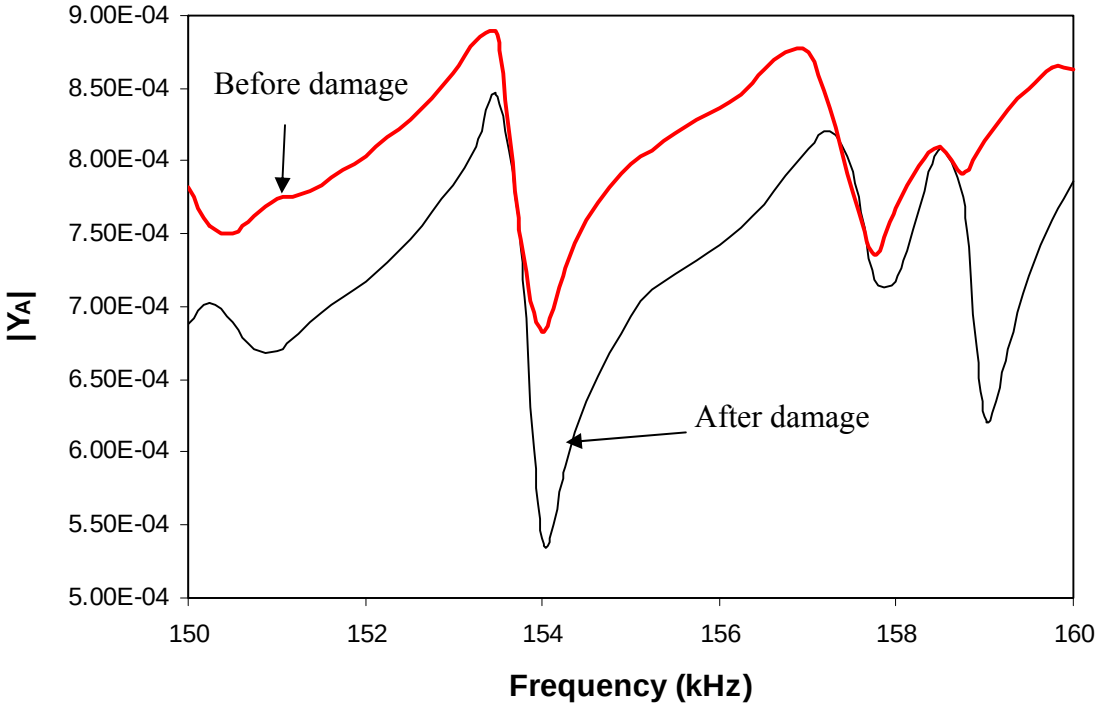

(b)

Fig. 15 Active admittance signatures before and after damage
(a) Using LCR meter (b) Using proposed low-cost hardware

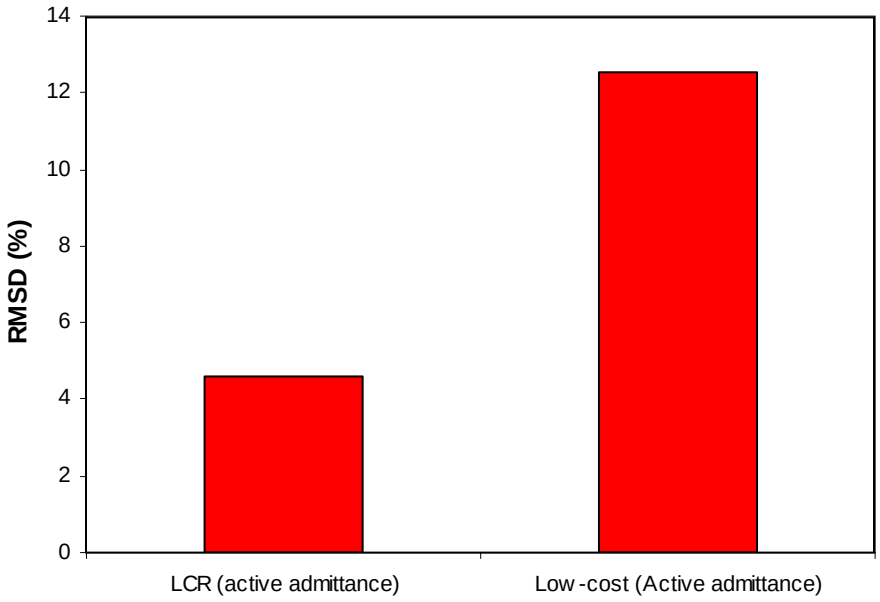

Fig. 16 Comparison of RMSD values for damage using LCR meter and low-cost EMI technique.